

Autonomous B-cell receptor signaling and genetic aberrations in chronic lymphocytic leukemia-phenotype monoclonal B lymphocytosis in siblings of patients with chronic lymphocytic leukemia

Edwin Quinten,^{1*} Julieta H. Sepúlveda-Yáñez,^{1,2*} Marvyn T. Koning,¹ Janneke A. Eken,¹ Dietmar Pfeifer,³ Valeri Nteleah,¹ Ruben A.L. de Groen,¹ Diego Alvarez Saravia,² Jeroen Knijnenburg,⁴ Hedwig E. Stuivenberg-Bleijswijk,¹ Milena Pantic,³ Andreas Agathangelidis,^{5,6} Andrea Keppler-Hafkemeyer,³ Cornelis A. M. van Bergen,¹ Roberto Uribe-Paredes,^{7,8} Kostas Stamatopoulos,^{6,9} Joost S.P. Vermaat,¹ Katja Zirlik,^{3,10} Marcelo A. Navarrete,² Hassan Jumaa¹¹ and Hendrik Veelken¹

¹Department of Hematology, Leiden University Medical Center, Leiden, The Netherlands;

²School of Medicine, Universidad de Magallanes, Punta Arenas, Chile; ³Department of Medicine I, University Medical Center Freiburg, Freiburg, Germany; ⁴Department of Clinical Genetics, Leiden University Medical Center, Leiden, The Netherlands; ⁵Department of Biology, School of Science, National and Kapodistrian University of Athens, Athens, Greece;

⁶Institute of Applied Biosciences, Center for Research and Technology Hellas, Thessaloniki, Greece; ⁷Department of Computer Engineering, Universidad de Magallanes, Punta Arenas, Chile; ⁸Center for Biotechnology and Bioengineering, Santiago, Chile; ⁹Department of Molecular Medicine and Surgery, Karolinska Institutet, Stockholm, Sweden; ¹⁰Tumor- und Brustzentrum Ostschweiz, Chur, Switzerland and ¹¹Institute of Immunology, University of Ulm, Ulm, Germany

*EQ and JHS-Y contributed equally as first authors.

Correspondence: H. Veelken
j.h.veelken@lumc.nl

Received: March 1, 2023.

Accepted: June 30, 2023.

Early view: July 13, 2023.

<https://doi.org/10.3324/haematol.2022.282542>

©2024 Ferrata Storti Foundation

Published under a CC BY-NC license



Supplemental Material to:

Autonomous BCR signaling and subclonal genetic variants in clonal CLL-phenotype B cells in siblings of CLL patients

Edwin Quinten, Julieta H. Sepúlveda-Yáñez, Marvyn T. Koning, Janneke A. Eken, Dietmar Pfeifer, Valeri Nteleah, Ruben A.L. de Groen, Diego Alvarez Saravia, Jeroen Knijnenburg, Hedwig E. Stuivenberg-Bleijswijk, Milena Pantic, Andreas Agathangelidis, Andrea Keppler-Hafkemeyer, Cornelis A. M. van Bergen, Roberto Uribe-Paredes, Kostas Stamatopoulos, Joost S.P. Vermaat, Katja Zirlik, Marcelo A. Navarrete, Hassan Jumaa, Hendrik Veelken

Supplemental Methods:

Patients, probands, and samples.

CLL patients under management of the outpatient clinics at the participating centers were asked to inform their respective living siblings about this study and to provide their contact information. Approvals by the ethical committees explicitly excluded longitudinal analyses and mandated to provide siblings with a categorical screening result.

Detection, isolation, and processing of CLL-phenotype cells

Differential blood counts were obtained for each blood sample. DNA and RNA were directly isolated from sorted CLL-phenotype cells by spun-driven silica matrix columns (Allprep DNA/RNA mini kit; Qiagen, Hilden, Germany).

Identification of clonal BCR transcripts

VDJ and VJ sequences were determined by direct Sanger sequencing from gel-purified ARTISAN PCR products (Wizard SV gel and PCR clean-up kit; Promega, Madison, WI) or after molecular cloning (Topo TA cloning vector; ThermoFisher, Waltham, MA).

Analysis of BCR signaling activity

pMIZCC and pMIZYN expression vectors¹ with inserted paired VDJ and VJ sequences from individual cases were synthesized (BaseClear BV, Leiden, The Netherlands) and packaged by liposomal cotransfection (FuGENE HD transfection reagent; Promega) of Phoenix-E cells with the pCL-eco helper vector. Murine TKO cells were transduced with virus-containing supernatant on fibronectin-coated plates at 48 h after transfection (RetroNectin; TaKaRa, Shiga, Japan).² TKO cells are arrested at the pro-B-cell stage by genetic deficiency of Rag2, Lambda5, and Slp65. Slp65 function is reconstituted by a Slp65-ERT2 fusion gene that enables BCR signaling in the presence of 4-hydroxytamoxifen.^{1,3}

Calcium mobilization was measured in Indo-1 AM-loaded (ThermoFisher), live-gated TKO cells by flow cytometry as the ratio of signal intensities (SIR) at 405 and 485 nm for 90 sec. After addition of 2 μ M 4-hydroxytamoxifen (Sigma Aldrich), calcium mobilization was measured for additional 7.5 min. Finally, maximum BCR signaling was induced by adding an unlabeled crosslinking anti-IgM or anti-IgG gamma antibody (clones 2022-01 and 2042-01; Southern Biotech, Birmingham, AL), and measurement was resumed for additional 3 min. Every BCR-transduced TKO population was measured at least twice at

approximately 3 and 4 weeks after transduction. The 2nd measurement was used for statistical analyses with two-tailed Mann-Whitney or Wilcoxon's rank sum tests for unpaired and paired comparisons, respectively, and Spearman's correlation coefficient.

Quantitative assessment of autonomous BCR signaling

The fraction of cells with a 405/485 SIR above the 95th percentile prior to addition of tamoxifen (Q^{aut}) was determined with correction for totally unresponsive cells during BCR crosslinking. Subsequently, the calibrated median SIR observed in this Q^{aut} fraction was determined ($\text{calSIR}^{\text{aut}}$). Autonomous BCR signaling was quantitated as the arithmetic product of $Q^{\text{aut}} \times \text{calSIR}^{\text{aut}}$.

Details of recording (see Figure):

Measurements of BCR signaling activity is performed in 3 phases:

1. Baseline Phase (BP): Time interval from the start of measurements until the addition of 4-hydroxytamoxifen
2. Experimental Phase (EP): Time interval from addition of tamoxifen until the addition of cross-linking agent
3. Maximum Phase (MP): Time interval from addition of cross-linking agent to the end of measurement

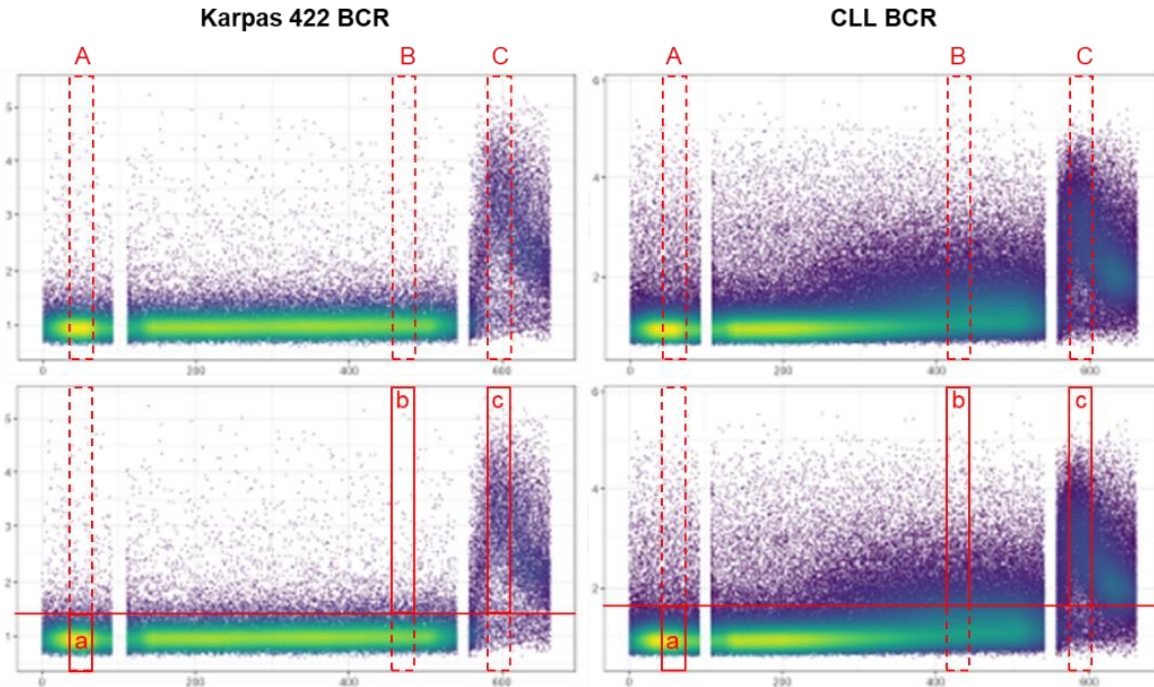
Three frames are defined and the number of events within each frame recorded:

- A. Frame A: Stable interval in BP with number of events = N_A
- B. Frame B: Stable interval towards the end of EP with number of events = N_B
- C. Frame C: Interval starting at the time point of maximum increase signaling intensity ratio (SIR) and covering the interval of peak SIR in MP with number of events = N_C .

Within each frame, a gate is defined and the number of events within each gate recorded:

- a) Gate a: Part of frame A with upper limit (=SIR95) set to contain 95% of all events within frame A = n_a
- b) Gate b: Part of frame B with lower limit set at SIR95 with number of events = n_b
- c) Gate c: Part of frame C with lower limit set at SIR95 with number of events = n_c

Mean SIR are recorded for gates b (SIR^b) and c (SIR^c).



Interpretation:

- The fraction of false-positive events is set to 0.05.
- The fraction of non-responsive cells is calculated as $(N_c - n_c) / N_c$.
- The fraction of cells with autonomous BCR signaling activity Q^{aut} with correction for 5% false-positive cells and fraction of unresponsive cells is calculated as:

$$Q^{aut} = (n_b N_c - 0.05 N_B N_c) / n_c N_c$$

- The calibrated autonomous BCR signal $calSIR^{aut}$ is: $calSIR^{aut} = SIR^b / SIR^c$
- BCR signaling strength is calculated as the product of the corrected fraction of cells with autonomous signalling and the calibrated autonomous BCR signal:

$$Q^{aut} calSIR^{aut}$$

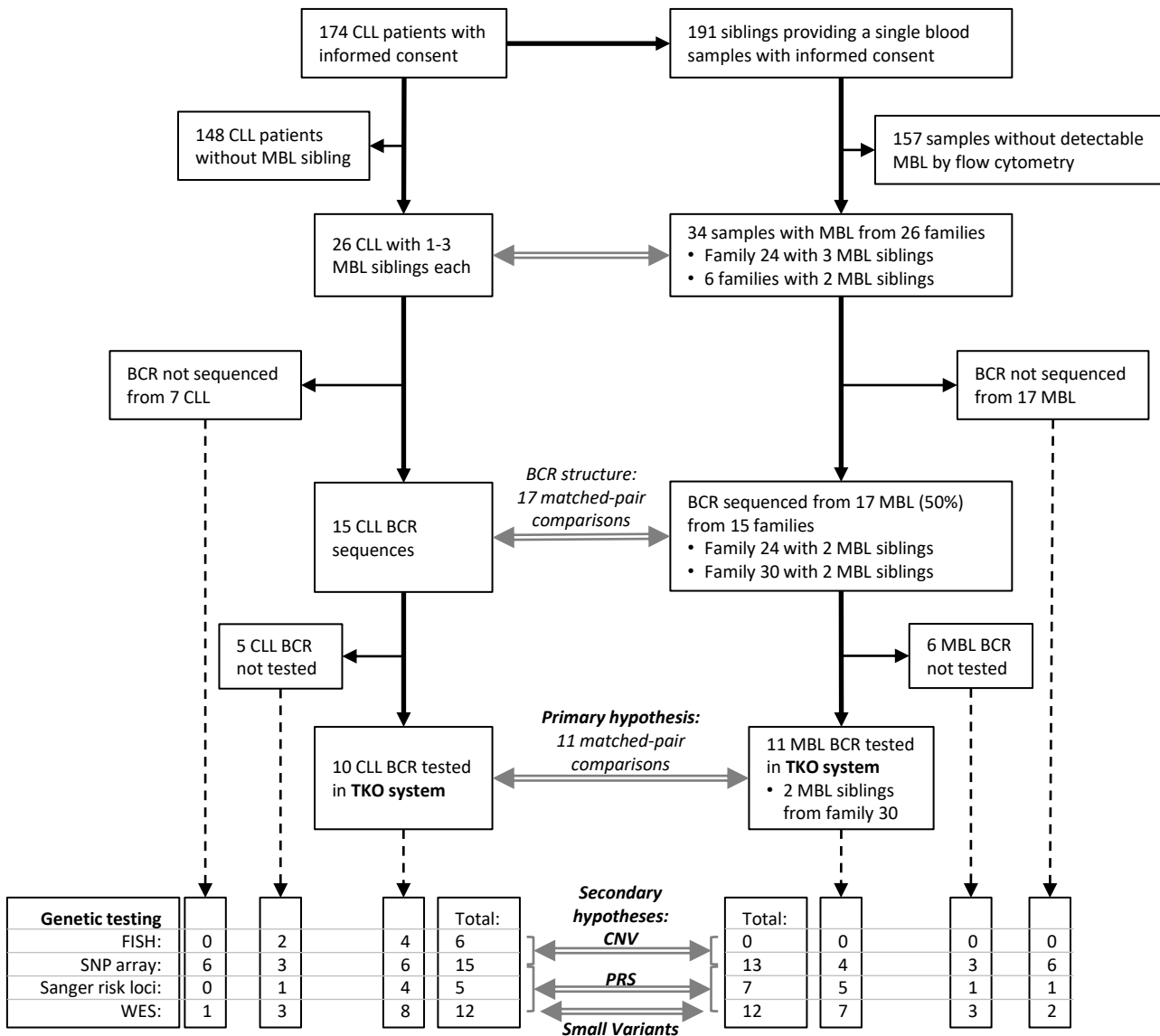
Whole Exome Sequencing

FASTQ files from whole exome sequencing (WES) were processed using the Sarek workflow v2.7 and aligned to the human reference genome GRCh38 using Burrows Wheeler Algorithm (BWA) v0.7.17.^{4, 5} Duplicated mapped reads were marked, local realignment of regions flanking indels and recalibration of base quality scores were performed to obtain more accurate bases according to the Genome Analysis ToolKit (GATK) best practices version v4.1.7.0.⁶ Single nucleotide variants (SNV) and short insertions and deletions (INDELS) were called using Strelka2 v2.9.10.⁷ Only high

confidence variants defined by quality scores (GQX) of at least 15 for SNV and 30 for INDELS were kept. The resulting variant call files were annotated by Ensembl-VEP (v103) with four filtering steps.⁸ Variants were first filtered for the 120 most frequent mutated genes in CLL according to the COSMIC database and an in-house cohort (Supplemental Table 3).^{9, 10} Thereafter, variants were filtered based on their effect, i.e. frameshift, in-frame deletion, missense, missense variant & splice region variant, splice region variant & synonymous variant, synonymous, in-frame insertion, stop gained, stop lost, frameshift variant & stop lost, missense variant & splice region variant, and coding sequence variant. Subsequently, variants were filtered for predicted deleterious effects using a CADD phred score of >20, and benign variants annotated in Clinvar 202008 were discarded. Workflow quality control metrics were calculated and aggregated by MultiQC v1.8.⁵ One sample (MBL24.3) with a high percentage (24.4%) of unmapped reads was discarded at this stage.

1. Duhren-von Minden M, Ubelhart R, Schneider D, et al. Chronic lymphocytic leukaemia is driven by antigen-independent cell-autonomous signalling. *Nature*. 2012;489(7415):309-312.
2. Maity PC, Bilal M, Koning MT, et al. IGLV3-21*01 is an inherited risk factor for CLL through the acquisition of a single-point mutation enabling autonomous BCR signaling. *Proc Natl Acad Sci U S A*. 2020;117(8):4320-4327.
3. Meixlsperger S, Kohler F, Wossning T, Reppel M, Muschen M, Jumaa H. Conventional light chains inhibit the autonomous signaling capacity of the B cell receptor. *Immunity*. 2007;26(3):323-333.
4. Garcia M, Juhos S, Larsson M, et al. Sarek: A portable workflow for whole-genome sequencing analysis of germline and somatic variants. *F1000Res*. 2020;9:63.
5. Li H, Durbin R. Fast and accurate short read alignment with Burrows-Wheeler transform. *Bioinformatics*. 2009;25(14):1754-1760.
6. McKenna A, Hanna M, Banks E, et al. The Genome Analysis Toolkit: a MapReduce framework for analyzing next-generation DNA sequencing data. *Genome Res*. 2010;20(9):1297-1303.
7. Kim S, Scheffler K, Halpern AL, et al. Strelka2: fast and accurate calling of germline and somatic variants. *Nat Methods*. 2018;15(8):591-594.
8. McLaren W, Pritchard B, Rios D, Chen Y, Flicek P, Cunningham F. Deriving the consequences of genomic variants with the Ensembl API and SNP Effect Predictor. *Bioinformatics*. 2010;26(16):2069-2070.
9. Morande PE, Yan XJ, Sepulveda J, et al. AID overexpression leads to aggressive murine CLL and nonimmunoglobulin mutations that mirror human neoplasms. *Blood*. 2021;138(3):246-258.
10. Tate JG, Bamford S, Jubb HC, et al. COSMIC: the Catalogue Of Somatic Mutations In Cancer. *Nucleic Acids Res*. 2019;47(D1):D941-D947.

Supplemental Figure 1:
 Consort-like diagram of numbers of samples and experimental analyses.
 CNV: Copy number variations. PRS: Polygenic risk score.



Supplemental Table 3: CLL-related genes analyzed for small variants

ADAM19	DLG2	LINGO2	PCLO
ADGRL2	DLGAP2	LRMDA	PDE4D
ADGRL3	DMD	LRP1B	PDIA4
AGBL1	DPP10	LRRTM4	PDZD3
AGBL4	DPP6	LUZP2	PRKCH
AKAP13	DSCAM	MACROD2	PRKG1
ANKS1B	EPHA5	MAGI2	PRKN
ASTN2	EPHA6	MCL1	PTPRD
ATM	ERBB4	MDGA2	PTPRN2
ATRNL1	EYS	MYD88	PTPRT
BIRC3	FAM155A	MYH15	RBFOX1
BRINP3	FAT3	NAALADL2	RIN3
CACNA2D1	FHIT	NAGPA	ROBO1
CACNA2D3	FSTL5	NCAM2	ROBO2
CCSER1	GABRG3	NCKAP5	ROS1
CDH12	GALNTL6	NEGR1	RYR2
CDH13	GPC5	NELL1	SEMA6D
CDH18	GPC6	NKAIN2	SF3B1
CELSR1	GREB1L	NLGN1	SGCZ
CNTN4	GRID2	NOTCH1	SH3TC1
CNTN5	GRIK2	NPAS3	SNTG1
CNTNAP2	GRM7	NRG3	SPAG16
CNTNAP5	H1-2	NRXN1	SPOCK3
CSMD1	H1-3	NRXN3	THSD7B
CSMD3	H1-5	OPCML	TP53
CTNNA2	IGLL5	PARD3B	UNC5D
CTNNA3	IL1RAPL1	PARP4	USH2A
CTNND2	IL1RAPL2	PAX5	XPO1
DCC	KCNIP4	PCDH11X	ZFHX3
DGKB	KLHL1	PCDH15	ZFPM2

Family	sample	CHROM	POS	SYMBOL	Gene	REF	ALT	QUAL	Allele	Consequence	IMPACT	cDNA_position	CDS_position	Protein_position	Amino_acids	Codons	Existing_variation
27	CLL27.1	chr2	197402635	SF3B1	ENSG00000115524	C	A	139	A	missense_variant	MODERATE	2027	1998	666	K/N	aaG/aaT	rs377023736&COSV59205777&COSV59205799
27	CLL27.1	chr8	1565843	DLGAP2	ENSG00000198010	C	A	572	A	missense_variant	MODERATE	1571	1391	464	P/Q	cCa/cAa	rs2301963&COSV70102130
27	CLL27.1	chr10	115334318	ATRNL1	ENSG00000107518	A	C	923	C	missense_variant	MODERATE	3460	3074	1025	N/T	aAt/aCt	rs1050159510
27	CLL27.1	chr11	99819645	CNTN5	ENSG00000149972	C	T	371	T	stop_gained	HIGH	688	157	53	R/*	Cga/Tga	rs12292659&COSV54311010
27	MBL27.1	chr4	161386160	FSTL5	ENSG00000168843	C	A	810	A	missense_variant	MODERATE	2533	2131	711	D/Y	Gat/Tat	rs3749598
27	MBL27.1	chr9	136515524	NOTCH1	ENSG00000148400	C	T	117	T	missense_variant	MODERATE	2124	1862	621	R/H	cGc/cAc	rs138504021&COSV99487877
27	MBL27.1	chr11	83962888	DLG2	ENSG00000150672	G	A	769	A	missense_variant	MODERATE	1723	1337	446	T/I	aCc/aTc	rs140599607
27	MBL27.2	chr1	215799051	USH2A	ENSG00000042781	G	T	1925	T	missense_variant	MODERATE	10253	9814	3272	P/T	Ccg/Acg	COSV100239515
27	MBL27.2	chr3	175737328	NAALADL2	ENSG00000177694	A	G	571	G	missense_variant	MODERATE	1993	1919	640	Q/R	cAa/cGa	rs62286105
27	MBL27.2	chr9	136523093	NOTCH1	ENSG00000148400	G	A	15	A	missense_variant	MODERATE	761	499	167	P/S	Cca/Tca	rs1439038323&COSV53077398
27	MBL27.2	chr13	24447125	PARP4	ENSG00000102699	T	C	54	C	missense_variant	MODERATE	3250	3176	1059	Q/R	cAg/cGg	rs77269056&COSV67960139
27	MBL27.2	chr13	24447185	PARP4	ENSG00000102699	A	G	194	G	missense_variant&splice_region_variant	MODERATE	3190	3116	1039	I/T	aTa/aCa	rs73172125&COSV67960144
28	CLL28.1	chr2	61492051	XPO1	ENSG00000082898	T	C	209	C	missense_variant	MODERATE	2672	1871	624	D/G	gAt/gGt	COSV68944745
28	CLL28.1	chr3	54569985	CACNA2D3	ENSG00000157445	G	A	672	A	missense_variant	MODERATE	931	769	257	V/M	Gtg/Atg	rs372465588&COSV55530096&COSV55536891
28	CLL28.1	chr5	157490332	ADAM19	ENSG00000135074	A	C	836	C	missense_variant	MODERATE	2297	2218	740	S/A	Tcc/Gcc	rs10067096&COSV57429259
28	CLL28.1	chr5	157509356	ADAM19	ENSG00000135074	T	C	462	C	missense_variant	MODERATE	929	850	284	S/G	Agt/Ggt	rs1422795&CM093420&COSV57425399
28	CLL28.1	chr5	157575687	ADAM19	ENSG00000135074	C	T	116	T	missense_variant	MODERATE	89	10	4	G/S	Ggc/Agc	rs11465228
28	CLL28.1	chr8	112636939	CSMD3	ENSG00000164796	A	G	695	G	missense_variant	MODERATE	3678	3593	1198	F/S	tTt/tCt	rs765163979
28	CLL28.1	chr15	85735078	AKAP13	ENSG00000170776	G	A	413	A	missense_variant	MODERATE	7576	7369	2457	G/S	Ggt/Agt	rs2241268&COSV63448267
28	MBL28.1	chr2	211630569	ERBB4	ENSG00000178568	T	A	238	A	missense_variant	MODERATE	2244	1972	658	I/F	Att/Ttt	rs190654033
28	MBL28.1	chr7	158138452	PTPRN2	ENSG00000155093	C	T	1271	T	missense_variant	MODERATE	1128	974	325	S/N	aGt/aAt	rs1130499&COSV67024020
28	MBL28.1	chr11	92797959	FAT3	ENSG00000165323	C	T	638	T	missense_variant	MODERATE	5320	4946	1649	P/L	cCg/cTg	rs375193261&COSV104590304&COSV53099591
28	MBL28.1	chr13	24447185	PARP4	ENSG00000102699	A	G	21	G	missense_variant&splice_region_variant	MODERATE	3190	3116	1039	I/T	aTa/aCa	rs73172125&COSV67960144
28	MBL28.1	chr13	91693325	GPC5	ENSG00000179399	C	T	367	T	missense_variant	MODERATE	890	464	155	A/V	gCg/gTg	rs553717&COSV65586039
28	MBL28.1	chr15	85580133	AKAP13	ENSG00000170776	G	A	764	A	missense_variant	MODERATE	2272	2065	689	E/K	Gag/Aag	rs7177107&COSV63448301
30	CLL30.1	chr2	124869717	CNTNAP5	ENSG00000155052	G	A	535	A	missense_variant	MODERATE	3752	3388	1130	V/I	Gta/Ata	rs1240405090
30	CLL30.1	chr11	100061213	CNTN5	ENSG00000149972	C	G	145	G	missense_variant&splice_region_variant	MODERATE	1513	982	328	P/A	Ccc/Gcc	rs201910584&COSV54330963
30	CLL30.1	chr13	24447185	PARP4	ENSG00000102699	A	G	63	G	missense_variant&splice_region_variant	MODERATE	3190	3116	1039	I/T	aTa/aCa	rs73172125&COSV67960144
30	CLL30.1	chr20	14085630	MACROD2	ENSG00000172264	C	T	133	T	missense_variant	MODERATE	568	173	58	T/I	aCt/aTt	rs2990505&COSV53960729
30	CLL30.1	chr22	22888259	IGLL5	ENSG00000254709	G	A	162	A	missense_variant&splice_region_variant	MODERATE	444	206	69	R/K	aGg/aAg	rs745485743&COSV73251123
30	MBL30.2	chr2	211722434	ERBB4	ENSG00000178568	G	T	367	T	missense_variant	MODERATE	1114	842	281	A/E	gCa/gAa	
30	MBL30.2	chr7	158138452	PTPRN2	ENSG00000155093	C	T	142	T	missense_variant	MODERATE	1128	974	325	S/N	aGt/aAt	rs1130499&COSV67024020
30	MBL30.2	chr15	85735078	AKAP13	ENSG00000170776	G	A	1813	A	missense_variant	MODERATE	7576	7369	2457	G/S	Ggt/Agt	rs2241268&COSV63448267
30	MBL30.1	chr1	81990901	ADGRL2	ENSG00000117114	G	A	326	A	missense_variant	MODERATE	4184	3968	1323	R/K	aGa/aAa	rs41292984&COSV54685119
30	MBL30.1	chr2	124524333	CNTNAP5	ENSG00000155052	C	T	416	T	missense_variant	MODERATE	1719	1355	452	S/L	tCg/tTg	rs17727261&COSV70497527
30	MBL30.1	chr2	137160352	THSD7B	ENSG00000144229	T	A	1207	A	missense_variant	MODERATE	1687	1509	503	D/E	gaT/gaA	rs4954474&COSV55680598
30	MBL30.1	chr13	24442624	PARP4	ENSG00000102699	G	A	230	A	missense_variant	MODERATE	3583	3509	1170	T/I	aCa/aTa	rs113301501&CM160622&COSV67960155
30	MBL30.1	chr18	21473100	GREB1L	ENSG00000141449	G	A	420	A	missense_variant	MODERATE	2080	1925	642	R/H	cGt/cAt	rs1343579561
30	MBL30.1	chr22	46364248	CELSR1	ENSG00000075275	A	C	22	C	missense_variant	MODERATE	9233	8783	2928	I/S	aTc/aGc	